Published in final edited form as:
J Neurosci. 2012 April 18; 32(16): 5385–5397. doi:10.1523/JNEUROSCI.6033-11.2012.

ADHD-Derived Coding Variation in the Dopamine Transporter Disrupts Microdomain Targeting and Trafficking Regulation

Dhananjay Sakrikar[1], **Michelle S. Mazei-Robison**[1,*], **Marc A. Mergy**[1], **Nathan W. Richtand**, **Qiao Han**[1], **Peter J. Hamilton**[2], **Erica Bowton**[2], **Aurelio Galli**[2], **Jeremy Veenstra-VanderWeele**[1,3], **Michael Gill**[4], and **Randy D. Blakely**[1,3]

[1]Department of Pharmacology, Vanderbilt University Medical Center, Nashville, TN 37232-8548 [2]Department of Molecular Physiology and Biophysics, Vanderbilt University Medical Center, Nashville, TN 37232-8548 [3]Department of Psychiatry, Vanderbilt University Medical Center, Nashville, TN 37232-8548 [4]Department of Psychiatry, Trinity Centre for Health Sciences, Dublin 8, Ireland

Abstract

Attention-Deficit Hyperactivity Disorder (ADHD) is the most commonly diagnosed disorder of school-age children. Although genetic and brain imaging studies suggest a contribution of altered dopamine (DA) signaling in ADHD, evidence of signaling perturbations contributing to risk is largely circumstantial. The presynaptic, cocaine and amphetamine (AMPH)-sensitive DA transporter (DAT) constrains DA availability at pre- and post-synaptic receptors following vesicular release and is targeted by the most commonly prescribed ADHD therapeutics. Using polymorphism discovery approaches with an ADHD cohort, we identified a human DAT (hDAT) coding variant, R615C, located in the transporter's distal C-terminus, a region previously implicated in constitutive and regulated transporter trafficking. Here we demonstrate that whereas wildtype DAT proteins traffic in a highly regulated manner, DAT 615C proteins recycle constitutively, and demonstrate insensitivity to the endocytic effects of AMPH and protein kinase C (PKC) activation. The disrupted regulation of DAT 615C parallels a redistribution of the transporter variant away from GM1 ganglioside- and flotillin1-enriched membranes, and is accompanied by altered calcium/calmodulin-dependent protein kinase II (CaMKII) and flotillin-1 interactions. Using C-terminal peptides derived from wildtype DAT and the R615C variant, we establish that the DAT 615C C-terminus can act dominantly to preclude AMPH regulation of wildtype DAT. Mutagenesis of DAT C-terminal sequences suggest that phosphorylation of T613 may be important in sorting DAT between constitutive and regulated pathways. Together, our studies support a coupling of DAT microdomain localization with transporter regulation and provide evidence of perturbed DAT activity and DA signaling as a risk determinant for ADHD.

Keywords

ADHD; dopamine; transporter; amphetamine; PKC; trafficking

Correspondence To: Randy D. Blakely, Ph.D., Vanderbilt Brain Institute, Suite 7140, MRBIII, Vanderbilt University Medical Center, Nashville, TN 37232-8548, Tel: 615-936-1700, FAX: 615-936-3745, randy.blakely@vanderbilt.edu.
*Current Address: Fishberg Department of Neuroscience, Mt. Sinai School of Medicine, New York, NY 10029

INTRODUCTION

The neurotransmitter DA provides critical modulatory influences over circuits subserving reward, locomotor activity, and attention (Carlsson, 1987, Robbins, 2003). As such, alterations in DA signaling contribute to multiple neurological and psychiatric disorders including Parkinson's disease (Chase et al., 1998), attention-deficit hyperactivity disorder (ADHD) (Mazei-Robison et al., 2005), and addiction (Ritz et al., 1987). The re-uptake of DA through presynaptic DATs is a primary mechanism for terminating DA action at presynaptic and postsynaptic receptors and is a major target for psychostimulants, such as cocaine and AMPH.

Multiple studies point to a contribution of variation in the genes encoding DAT, catechol-O-methyl transferase (COMT) and/or DA receptors as influencing risk for ADHD (Gill et al., 1997, Qian et al., 2003, Bobb et al., 2005, Mazei-Robison et al., 2005), the most commonly diagnosed disorder of school age children in the U.S. A further link between DAT function and ADHD is suggested from the therapeutic utility of DAT-interacting psychostimulants, including methylphenidate (Ritalin®) and AMPH preparations (e.g. Adderall®). Brain imaging studies also point to deficits in DA signaling as a key feature of ADHD (Swanson et al., 2007). Genetic elimination of DAT expression in mice reduces presynaptic DA stores, elevates extracellular DA, and produces hyperactivity in a novel environment (Giros et al., 1996). However, humans that are homozygous for loss of function DAT (*SLC6A4*) alleles exhibit infantile neonatal dystonia rather than ADHD (Kurian et al., 2009), raising questions as to the relevance of compromised DAT function and DA signaling as a key feature in ADHD.

Reasoning that genetic alterations that perturb DAT regulation, as opposed to DAT elimination, could reconcile data from rodent and human studies, we screened ADHD subjects for rare variation producing coding variation in DAT. Previously, we described the anomalous, non-vesicular release of DA by the DAT A559V coding variant (Mazei-Robison et al., 2008), leading to the hypothesis that dysregulated DA availability may be a determinant of risk for ADHD. Here we provide additional evidence for this idea through study of the properties of a second DAT variant, R615C. Our studies reveal novel contributions of the DAT C-terminus in orchestrating the transporter's membrane compartmentalization, trafficking pathways and protein associations. The functional impact of the DAT R615C variant on DAT localization and trafficking encourages further evaluation of perturbations of DAT regulatory networks in ADHD.

MATERIALS AND METHODS

Materials

DMEM and FBS were from Gibco. Mouse anti CaMKII antibody (MA1-048), TCEP, Sulpho-NHS-SS-Biotin, and streptavidin agarose resin were from Thermo Fisher. [^{3}H] DA and [^{32}P] orthophosphoric acid were from PerkinElmer. Alexa Fluor 647 CTxB was from Invitrogen. KN-93, KN-92 and β-PMA were from EMD biosciences. Rat and rabbit anti-hDAT antibodies were from Millipore (MAB369 and AB5803 respectively). Mouse anti-flotillin-1 antibody was from BD Biosciences (Catalog # 610820). Secondary antibodies were obtained from Jackson Laboratories. Other reagents were obtained from Sigma.

ADHD subject collection and ascertainment

Subject recruitment and ascertainment for U.S. ADHD probands has been previously described (Mazei-Robison et al., 2005, Mazei-Robison et al., 2008). Additional subjects from Ireland were also enrolled from child guidance clinics and ADHD support groups around Ireland. The age range of the probands was between 5 and 14 years, with males

accounting for 88% of the cases. To establish DSM-IV diagnoses, one or both parents were interviewed using the Child and Adolescent Psychiatric Assessment (CAPA). To fulfill DSM-IV ADHD criteria for symptom pervasiveness, information regarding ADHD symptoms at school was obtained from teachers using a semistructured teacher telephone interview. ADHD symptom dimensions, as well as comorbid disorders such as Oppositional Defiant Disorder (ODD) and Conduct Disorder (CD) were obtained from the Child and Adolescent Psychiatric Assessment (CAPA). A positive family history of ADHD was defined by at least one parent scoring 36 or greater on the 25 item subscale of the Wender Utah Rating Scale (WURS). A 25-item sub scale was used in with a cutoff score of 36 or greater being 96% sensitive and specific for a retrospective diagnosis of childhood ADHD in the parent.

PCR amplification of hDAT exons and polymorphisms screening via temperature gradient capillary electrophoresis (TGCE)

PCR amplification, screening and sequence confirmation was performed as described previously (Mazei-Robison et al., 2005).

Cell culture, transfections, and stable cell line generation

Flp-In™ 293 cells were used to generate stable lines expressing either DAT 615R or DAT 615C following the manufacturer's protocol (Invitrogen™). Selection media contained 100 μg/ml Hygroycin B. HEK 293T cells used for transient transfections were cultured, maintained and transfected as described previously (Mazei-Robison and Blakely, 2005).

DA transport assays

[^{3}H] DA transport assays were performed in triplicate or quadruplet in 24 well plates as described previously (Apparsundaram et al., 1998). Briefly, cells were washed with Krebs-Ringers-HEPES (KRH) (130 mM NaCl, 1.3 mM KCl, 2.2 mM $CaCl_2$, 1.2 mM $MgSO_4$, 1.2 mM KH_2PO_4, 10 mM HEPES, pH 7.4) buffer and were incubated in the uptake assay buffer (KRH, 10 mM glucose, 100 μM pargyline, ascorbic acid, and 10 μM tropolone) before incubation with [^{3}H] DA for 10 min followed by three 4°C washes. To determine non-specific uptake, parallel wells were incubated with 1 μM GBR 12909 5 min prior addition of [^{3}H] DA. For single point uptake assays, 50 nM [^{3}H] DA was used. For saturation kinetic analyses, six different DA concentrations were used (0.05, 0.1, 0.5, 1, 2, and 3 μM or 0.05, 0.1, 0.5, 1, 3, and 6 μM). Serial dilution from a stock made with 5% [^{3}H] DA was used for saturation analyses, except for the 50 nM concentration where 100% tritiated substrate was used. For all inhibitors, six concentrations (0.001, 0.01, 0.1, 0.5, 1, 10 μM) were tested to determine IC_{50} values. With AMPH treatments, cells were rapidly washed with ice-cold KRH buffer and warmed back up to 37°C using uptake assay buffer for 5 min before addition of [^{3}H] DA for a further 3 min incubation. The shorter uptake time was used to reduce confounds from DA efflux due to the presence of intracellular AMPH. MicroScint scintillation cocktail was added to the wells at the end of the assay and DA uptake was measured using a TopCount Scintillation Counter. Mean +/− SEM values reported derive from 3–6 independent experiments.

Cell surface biotinylation, biotinylation internalization, and biotinylation recycling assays

Cells were seeded in 6 well plates and incubated for 36–48hrs before experiments. Cells were washed twice with warm KRH buffer before drug treatments. At the end of the treatment time, cells were placed on ice and washed rapidly twice with ice-cold PBS (136 mM NaCl, 2.5 mM KCl, 1.5 mM KH_2PO_4, 6.5 mM Na_2PO_4, 2.8 mM glucose) containing 0.1mM $CaCl_2$ and 1mM $MgSO_4$ Cells were incubated with sulphosuccinimidyl-1-2-(biotinamido)ethyl-1,3-dithioproprionate-biotin (Sulpho-NHS-SS-Biotin) for 30 min at 4°C.

Excess biotin was quenched by 2 washes with 0.1 M glycine in PBS and cells were solubilized using radioimmunopreciptation assay (RIPA) (100 mM Tris pH 7.4, 150 mM NaCl, 1 mM EDTA, 0.1 % SDS, 1 % TritonX-100, 1 % sodium deoxycholate) buffer for 30 min at 4°C.

To determine the internalization rate, we used a modified version of a previously published protocol (Holton et al., 2005). Briefly, cells seeded on 2 different plates were labeled with Sulpho-NHS-SS-Biotin for 30 min at 4°C and quenched with 0.1 M glycine in PBS. One plate was mainlined at 4°C to determine total surface expression and stripping efficiency. The other plate was warmed by 3 rapid washed with warm PBS and cells were incubated with warm PBS at 37°C for 30 min either with or without AMPH to allow trafficking of the surface proteins. At the end of incubation, plates were transferred onto ice and cells and washed 3 times with ice-cold PBS followed by 3 washes with NT buffer (150 mM NaCl, 1 mM EDTA, 0.2% BSA, 20 mM Tris pH 8.6). The biotin signal remaining on the surface from the 37°C plates and stripping control wells from 4°C plates were stripped using 50 mM tris(2-carboxyethyl)phosphine (TCEP) in NT buffer for 60 min at 4°C. Fresh stripping solution was added after the first 30 min to ensure optimal stripping efficiency. Cells were washed rapid three times with ice-cold NT buffer followed by ice-cold PBS and solubilized using RIPA buffer for 30 min at 4°C. Protein concentration was determined using the BCA protein assay and equal protein amounts were incubated with pre-washed streptavidin beads for 2hr or overnight at 4°C. Streptavidin beads were washed three times with RIPA buffer and bound proteins were eluted using Laemmli sample buffer (LSB) and analyzed using SDS-PAGE, followed by western blotting. A rat anti-hDAT antibody (Millipore-MAB 369, 1:5000) was used to visualize DAT and mouse anti β-actin (Sigma-a5316, 1:5000) antibody was used to detect β-actin as a loading control. HRP-conjugated goat anti rat and mouse secondary antibodies (1:10000) were used.

Recycling rates were estimated using a biotinylation-recycling assay. Cells were labeled with Sulpho-NHS-SS-Biotin for 60 min at 37°C to achieve labeling of both surface and recycling intracellular proteins. Cells were placed on ice and cooled by washing with ice-cold PBS, followed by NT buffer three times each. Surface biotin labeling was stripped using 50 mM TCEP in NT buffer for 90 min at 4°C. After an initial 60 min of stripping, fresh TCEP solution was added for the remaining 30 min to ensure efficient stripping, assessed via western blots. Following stripping, cells were washed rapidly three times with ice-cold NT buffer followed by three times with ice-cold PBS buffer. One plate was maintained at 4°C, and the other plate was warmed by washing three times with 37°C PBS. Cells were then incubated for 30 min either with or without AMPH at 37°C. At the end of the incubation, cells were again placed on ice and washed three times with ice-cold PBS followed by NT buffer. Biotin signal from intracellular DAT that recycled to the surface was stripped by incubating cells in 50 mM TCEP in NT buffer on ice for 60 min, with fresh stripping buffer added after 30 min. Cells were then washed three times with ice-cold NT buffer followed by three washes with ice-cold PBS buffer and solubilized using RIPA buffer for 30 min at 4°C. Streptavidin pulldown and western blots were performed as described above.

Co-immunoprecipitation (co-IP) assays

DAT-CaMKII co-IP—HEK 293T cells were seeded on 10 cm dishes and co-transfected with pEYFP-HA-hDAT-WT (615R) (gift from Dr. Alexander Sorkin) or the pEYFP-HA-hDAT 615C variant and CaMKIIα (gift from Dr. Roger Colbran) 24hrs later. The pEYFP-HA-hDAT-WT construct has an N-terminal YFP tag and the HA tag derives from modifications of extracellular loop 2, as described elsewhere (Sorkina et al., 2003, Sorkina et al., 2006). The presence of YFP- or HA- tag does not interfere with expression, function

and trafficking of DAT (Sorkina et al., 2006). Cells were lysed using co-IP buffer (50 mM Tris pH 7.4, 150 mM NaCl, 1% TritonX-100) containing protease inhibitors 48hr post-transfection. Immunoprecipitation was performed overnight using goat anti CaMKII antibody (gift from Dr. Roger Colbran) and co-immunoprecipitated DAT was visualized using rat anti-hDAT antibody as for western blots noted above. Mouse anti-CaMKII antibody (1:5000) was used to visualize immunoprecipitated CaMKII. Goat IgG was used in parallel co-IP experiments to insure specificity of immunoprecipitation.

DAT-flotillin-1 co-IP—Flp-in™ HEK stable cells were seeded on 10 cm dishes. Cells were lysed using co-IP buffer 48hr after plating. Immunoprecipitation was done using rat anti-hDAT antibody and co-precipitated flotillin-1 was visualized using a mouse anti flotillin-1 antibody (1:1000). Rabbit anti-hDAT antibody (1:5000) was used to visualize immunoprecipitated DAT. Extracts from Flp-In HEK parent line were used as a negative control.

Metabolic labeling to assess DAT phosphorylation

[^{32}P] orthophosphate metabolic labeling was performed as described previously (Bowton et al., 2010). Briefly, Flp-In HEK stable cells were seeded on 6 well plates and cultured for 48hrs. Cells were washed once with phosphate free DMEM and incubated in the same medium for 1hr pool at 37°C to deplete the intracellular ATP. Cells were then supplemented with 1 mCi/ml of [^{32}P] orthophosphoric acid and incubated for 4hrs at 37°C. Cells were then washed 3 times with ice-cold PBS and lysed with RIPA buffer containing protease inhibitors and 1 μM okadaic acid and microcystin each for 30 min at 4°C. Lysates were immunoprecipitated with rat anti-DAT antibody overnight at 4°C. Immunoprecipitated DATs were visualized using SDS-PAGE, followed by autoradiography and densitometry.

Cholera toxin B (CTxB) labeling and confocal microscopy

HEK 293T cells were plated on glass bottom MatTek plates. Cells were transfected with pEYFP-HA-hDAT-WT (615R) or pEYFP-HA-hDAT 615C 24hrs later and cultured for 48 hrs. Cells were washed 3 times with ice-cold PBS containing 0.1 mM $CaCl_2$ and 1 mM $MgSO_4$ and incubated with 1 μg/mL Alexa 647 conjugated CTxB for 30 min at 4°C. Cells were washed 3 times with ice-cold PBS and fixed using 4% paraformaldehyde for 10 min at room temperature. Fixed cells were washed with PBS and stored in PBS until imaging at 4°C. Confocal imaging was performed in the VUMC Cell Imaging Shared Resource (supported by NIH grants CA68485, DK20593, DK58404, HD15052, DK59637 and EY08126). Laser output was adjusted to assure that all fluorescence monitored was non-saturating with respect to fluorophore emission. Intensity correlation quotient (ICQ) to assess colocalization of DAT with CTxB labeled membranes was obtained as previously described (Steiner et al., 2009, Baucum et al., 2010) using the Integration Colocalization Analysis section of WCIF Image J http://www.uhnresearch.ca/facilities/wcif/imagej/. This analysis computes a correlation in the intensity of two probes across pixels in regions of interest, with ICQ values distributed between −0.5 and +0.5. ICQ values that report evidence for colocalization fall between 0 and + 0.5 and are evaluated for significance using a One sample t-test comparing against a zero ICQ value. Genotype differences in ICQ values were determined by a two tailed, Student's t-test.

Detection of AMPH using High-Pressure Liquid Chromatography (HPLC)

Flp-In HEK cells were seeded in 6 well plates and incubated for 36–48hrs before experiments. Cells were washed twice with warm KRH buffer before incubation with 10 μM AMPH for 5 minutes at 37°C. Cells were rapidly washed 3 times using ice-cold KRH buffer and lysed using 10 mM TRIS/1 mM EDTA, pH 8.0 buffer (TE) containing protease

inhibitors. Total protein concentration was determined using BCA protein assay and used to normalize the AMPH uptake. AMPH uptake was determined using HPLC analysis and data are expressed as nmol AMPH transported per μg protein.

Amperometry

Unpatched amperometric currents were recorded as previously described(Bowton et al., 2010) using Flp-In™ HEK stable cells. Briefly, cells were plated at a density of 10^3 per 35-mm culture dish. To preload cells with DA, attached cells were washed with KRH assay buffer containing 10 mM D-glucose, 100 μM pargyline, 1 mM tropolone, and 100 μM ascorbic acid, and then incubated with 1 μM DA in assay buffer for 20 min at 37°C. Dishes containing DA loaded cells were then washed three times with external solution (130 mM NaCl, 10 mM HEPES, 34 mM D-glucose, 1.5 mM $CaCl_2$, 0.5 mM $MgSO_4$, 1.3 mM KH_2PO_4, adjusted pH to 7.35, and 300 mOsm). A carbon fiber electrode (ProCFE; fiber diameter of 5 μm; obtained from Dagan Corporation), juxtaposed to the plasma membrane and held at +700 mV (a potential greater than the oxidation potential of DA), was used to monitor basal and AMPH-evoked DA efflux through DAT as a consequence of DA oxidation. To determine basal DAT-dependent efflux, cells were treated with 10 μM cocaine following establishment of a stable recording baseline. Cells were not voltage-clamped in basal or AMPH (10 μM)-evoked DA efflux experiments. Amperometric currents in response to an addition of AMPH were recorded using an Axopatch 200B amplifier (Molecular Devices, Union City, CA) with a low-pass Bessel filter set at 1 kHz. Traces were digitally filtered offline at 1 Hz using Clampex9 software (Molecular Devices). DA efflux was quantified as the mean peak amperometric current (in picoamperes) +/− SEM.

Quantification and statistics

Western blots were quantified using NIH Image J software, with multiple exposures taken to insure linearity of signal detection. Student's t-test or one-way ANOVA with Bonferroni's post hoc test was used wherever appropriate. GraphPad Prism was used to determine V_{max} and K_m for saturation kinetic analyses and IC_{50} for inhibition analyses. Significant differences between DAT 615R and 615C values of V_{max}, K_m, and IC_{50} were determined using Student's t-test and a *P* value of 0.05 was considered as evidence of significance.

RESULTS

Identification of a functional DAT coding variant in an ADHD subject

Using polymorphism discovery methods (Li et al., 2002), we screened coding exons and intron-exon junctions of the *SLC6A4* gene in 417 ADHD subjects. Although a number of variants have been identified that alter the coding of DAT, all known variants are rare (allele frequency <1%) (Mazei-Robison et al., 2005). In an Irish cohort of 100 subjects receiving a DSM-IV diagnosis of ADHD (Bellgrove et al., 2009), we identified a nonsynonymous, single nucleotide polymorphism (SNP, 2026 T/C) that converts a highly conserved Arg residue at position 615 to Cys (R615C). R615 is completely conserved in mammalian DATs and resides in a generally well-conserved region of the DAT C-terminus (Fig. 1A), a region implicated in transporter somatic export, surface trafficking and protein-protein interactions (Torres et al., 2001, Bjerggaard et al., 2004, Fog et al., 2006). The subject, a Caucasian male of European origin, 13 years old at the time of assessment, had a strong clinical and research diagnosis of combined type ADHD (Connor's parent rating scale-inattentive symptoms, T=70; hyperactive symptoms, T=75, total score=74, WISK-III UK IQ=141) and was found to be heterozygous for the R615C variant. Pedigree genotyping revealed that the mutation was transmitted from the proband's mother who is retrospectively suspected to have suffered from ADHD as a child (Wender-Utah=59), though no clinical diagnosis is currently available. The subject's father and two older sisters who do not carry the variant are

unaffected (Fig. 1B). The R615C proband has been successfully treated with methylphenidate.

To search for functional evidence that the R615C variant may be causal in the proband's ADHD, we compared the activities of DAT 615R and DAT 615C in stably transfected HEK cells. To limit confounds associated with different sites of integration, we created stable Flp-In™ HEK lines that express either of the two transporters from a common locus, under the control of the same promoter (Sauer, 1994). Saturation kinetic analysis revealed a significant reduction in DA transport V_{max} for the R615C variant (615R, 1.6±0.2 vs. 615C, 1.0±0.1 pmol/μg protein/min, $P<0.005$, two-tailed Student's t-test) without a significant change in DA K_m (1.3±0.4 vs. 1.0±0.3 μM) (Fig. 1C). The reduced DA transport capacity was associated with a reduction in steady-state DAT protein levels (86±3% of DAT 615R; n=6, $P<0.005$, two-tailed Student's t test) and diminished surface transporter expression (50±7% of DAT 615R; n=6, $P<0.0001$, two-tailed Student's t test) (Fig. 1D), the latter determined by whole cell biotinylation. However, we observed no significant differences in the IC_{50} values for cocaine (615R, 7.7±2.0 vs. 615C, 10.0±2.1 nM), GBR 12909 (615R, 9.7±3.0 vs. 615C, 10.9±2.0 nM), or AMPH (615R, 329±135 vs. 615C, 226±101 nM), and a small, but statistically significant loss of potency for methylphenidate (615R 585±290 vs. 615C, 821±160 nM, $P<0.05$, two-tailed Student's t-test). Thus, although surface levels and DA transport capacity are reduced, the R615C variant exhibits normal interactions with DA and DAT antagonists.

Anomalous modulation of DAT 615C by AMPH

AMPH produces two alterations in DAT-expressing cells (Sulzer et al., 2005). First, AMPH induces (sec-min) nonvesicular DA release (efflux), mediated by reverse transport of cytoplasmic DA supported by CaMKII-mediated phosphorylation of the DAT N-terminus (Khoshbouei et al., 2003, Fog et al., 2006). Second, AMPH treatment of DAT-expressing cells has been reported to produce both a rapid translocation of the transporter to the cell surface (Furman et al., 2009), and, with more prolonged treatment (10–30 min), produces net transporter internalization (Saunders et al., 2000, Chen et al., 2010). Using carbon fiber amperometry (Bowton et al., 2010) we monitored basal efflux from DAT 615R and DAT 615C cells preloaded with DA (data not shown), and found no significant difference. We also monitored AMPH-triggered DA efflux from DA-preloaded cells and, as shown in Fig. 2A, 615R and 615C expressing cells exhibited comparable AMPH-evoked DA efflux, measured using the peak amplitude of amperometric responses. This finding was surprising due to the reduced steady-state DAT surface expression of the R615C variant noted above. We found a possible answer to this conundrum in examining the impact of AMPH on transporter surface expression. Whereas treatment of 615R expressing cells with 10 μM AMPH for 30 min produced the expected reduction in transporter surface expression, without any change total DAT protein levels (Fig. 2B), the same treatment failed to reduce surface expression of DAT 615C. Consistent with these findings, AMPH reduced DA transport from DAT 615R cells, but not from DAT 615C cells (Fig. 2C). Equivalent findings were also obtained following transient transfection of DAT 615R or DAT 615C into HEK-293T cells (data not shown) or CAD cells, a catecholamine-producing neuronal cell line (Qi et al., 1997) (Fig. 2D, E). DAT internalization is known to occur following PKC activation via phorbol esters, such as β-PMA(Loder and Melikian, 2003). We also found that the DAT 615C displayed no net endocytosis (109±9% of vehicle treated cells) and displayed no reduction in DA transport activity (98±2% of control), following β-PMA treatment (200 nM, 30 min). On the other hand, similar β-PMA treatment caused internalization of DAT 615R (72±4% of vehicle treated cells, $P<0.005$, two-tailed Student's t-test) and a significant reduction in DA transport activity (61±6% of control, $P<0.001$, two-tailed Student's t-test)"

AMPH modulates DAT trafficking upon entering the cell, as demonstrated by studies of a transport incompetent DAT mutant where intracellular injection of AMPH causes transporter internalization (Kahlig et al., 2006). Possibly, the R615C variant could transport AMPH more efficiently than wildtype DA, leading to the appearance of equivalent DA efflux despite reduced surface expression. However, HPLC assays of DAT 615C cells treated with AMPH under the same conditions used for efflux assays revealed similar levels of intracellular AMPH for DAT 615R and DAT 615C cells (615R, 4.9±1.5 nM vs. 615Cm 5.1±1.5 nM, n=4, P>0.05, two-tailed Student's t-test).

DAT R615C exhibits accelerated rates of constitutive endocytosis and recycling

To define the mechanisms supporting loss of AMPH-induced surface trafficking of the DAT R615C variant, we implemented kinetic surface biotinylation assays that report rates of membrane protein endocytosis and recycling (Deken et al., 2003, Holton et al., 2005). By monitoring the amount of surface biotinylated DAT that displays resistance to a biotin-stripping reagent, we quantified the extent of transporter internalization under basal and AMPH-treated conditions. Here, we discovered that the DAT R615C variant displays an accelerated, constitutive internalization rate relative to the wildtype transporter (Fig. 3A). Moreover, whereas AMPH significantly increased the rate of internalization for wildtype DAT, we observed no change in DAT 615C internalization rate over that seen under basal conditions.

Possibly, accelerated internalization of DAT 615C under basal conditions might explain its significantly diminished basal surface expression. Alternatively, a change in surface recycling could also explain this difference, and also account for insensitivity to AMPH. We therefore determined the extent of DAT 615R and 615C recycling by biotinylating the full pool of recycling transporter molecules at 37°C, followed by stripping away any surface resident transporters at 4°C. Upon warming the cells back to 37°C, we determined the rate of reappearance of either wildtype or DAT 615C. Thirty minutes after stripping and shifting back to 37°C, approximately 40% of wildtype DAT remained intracellular under basal conditions, and the extent of recycling was not further decreased by AMPH. In contrast, approximately 90% of the DAT R615C variant recycled under basal conditions. This capacity for recycling was also not diminished by AMPH (Fig. 3B). Thus, AMPH treatment produced a net internalization of wildtype DAT protein by enhancing transporter endocytosis rates without a compensatory increase in recycling rates. DAT 615C constitutively endocytosis and recycles at a much faster rate than wildtype transporters, and this difference is not impacted by AMPH treatment. Thus, the failure of DAT 615C to exhibit AMPH-triggered internalization and a commensurate reduction in DA uptake (Fig. 2B,C) is due to the transporter's efficient recycling through a pathway that cannot support acceleration of trafficking rates, which are already elevated.

DAT 615C reveals a CaMKII-dependent state of functional inactivation

AMPH acts to mobilize intracellular calcium (Ca^{2+}) in a CaMKII-dependent manner (Gnegy et al., 2004, Wei et al., 2007) and Ca^{2+} mobilization/CaMKII activation has been shown to be critical for AMPH evoked DA efflux, likely through phosphorylation of the DAT N-terminus (Khoshbouei et al., 2004a, Fog et al., 2006). Most relevant to our trafficking studies, CaMKII inhibition has also been shown to preclude net AMPH-mediated DAT surface redistribution (Wei et al., 2007). Since DAT 615C effluxes DA in response to AMPH, yet fails to traffic, we investigated whether CaMKII/DAT interactions, which depend on residues 615–617, remain intact (Fog et al., 2006). As shown in Fig. 4A, we detected an ~2 fold increase in recovery of DAT 615C/CaMKII vs. 615R/CaMKII complexes. Since CaMKII binding to the DAT C-terminus results in phosphorylation of DAT N-terminal serines (Fog et al., 2006), we asked whether the increased CaMKII

association of the R615C variant is paralleled by a change in transporter phosphorylation. Indeed, immunoprecipitation of DAT 615R or 615C from [^{32}P] orthophosphate labeled cells revealed a significantly increased basal phosphorylation of the R615C variant (Fig. 4B) when data were normalized by total protein input. Given that, in the stable cell lines used, total DAT 615C protein levels are modestly, but significantly reduced when compared to total WT DAT protein, the elevation in DAT 615C phosphorylation is likely to be actually somewhat higher than illustrated.

To assess whether the increased CaMKII association and basal phosphorylation associated with the R615C variant has functional consequences, we treated DAT 615R or 615C cells with the CaMKII inhibitor KN-93, either by itself, or as a pretreatment before AMPH addition. Treatment of cells with KN-93 alone did not impact the DA transport activity of wildtype, 615R cells (Fig. 5A). However this treatment blocked the reduction imposed on DA transport activity by AMPH treatment. As shown above, AMPH imposed no significant effect on DA transport activity for DAT 615C cells (Fig. 5A). Surprisingly, KN-93 alone significantly decreased the DA transport activity of 615C cells and this effect was more pronounced combining KN-93 with AMPH. The specificity of these drug treatments was confirmed through the use of KN-92, a structural analog of KN-93 that does not inhibit CaMKII (Fig. 5B). Thus it is possible that excessive, constitutive CaMKII regulation of DAT 615C contributes to the shift of transporters to an AMPH-insensitive endocytosis and recycling pathway. Indeed, biotinylation studies demonstrated that CaMKII blockade with KN-93 antagonized AMPH-induced reductions in cell surface expression cell of wildtype DAT (Fig. 5C), similar to its ability to block AMPH-induced reductions in DA uptake. In contrast to its effect on DAT 615C-supported DA uptake, KN-93 treatment produced no effect on transporter internalization alone or in the presence of AMPH (Fig. 5C). These data reveal a CaMKII-dependent capacity to modify the function of DAT R615C in a trafficking-independent manner.

The ability of CaMKII to enhance DAT 615C DA transport activity could arise from either a shift of transporters to high-affinity DA recognition or from a concentration-independent increase in DA transport capacity. To address these possibilities, we conducted saturation kinetic analysis for the DAT R615C variant, in the presence or absence of KN-93+AMPH (Fig. 5D). These drug treatments produced no significant change in DA transport K_m (basal, 5.4±1.5 vs. KN-93+AMPH, 3.8±0.6 μM), but generated a significant reduction in DA transport V_{max} (basal, 65±10 vs. KN-93+AMPH, 42±4 pmol/well/min, $P<0.05$, two-tailed Student's t-test). These findings support the hypothesis that CaMKII activity is required to sustain R615C in an active state.

DAT 615C demonstrates altered localization to membrane microdomains

Membrane microdomains have been reported to associate with (Foster et al., 2008) and influence DAT conformations (Hong and Amara, 2010), to constrain DAT lateral mobility (Adkins et al., 2007), to be required for PKC-mediated internalization, and to dictate CaMKII-mediated DA efflux (Cremona et al., 2011). DAT has been shown to localize to microdomains enriched for the protein flotillin-1(Cremona et al., 2011). Co-immunoprecipitation studies revealed reduced levels of the flottilin-1 in extracts of cells stably transfected with DAT 615C versus extracts from cells transfected with wildtype DAT (Fig. 6A). Since reduced association of flotillin-1 could reflect diminished surface expression of DAT (no data has been published as to whether DAT/flotillin-1 associations are present in recycling endosomes or limited to the plasma membrane), as opposed to a change in microdomain localization, we used confocal imaging to compare the colocalization of YFP-tagged DAT 615R or 615C proteins with Alexa 647-conjugated cholera toxin B subunit (CTxB). The latter probe detects GM1 ganglioside, another molecule known to localize to discrete membrane subdomains (Simons and Ikonen, 1997).

Moreover, in transfected N2a cells, DAT has been found to exhibit a greater degree of colocalization with CTxB labeled membranes, when compared to the transferrin receptor (Adkins et al., 2007). As shown in Fig. 6B, colocalization of the DAT R615C variant with CTxB labeled membranes was significantly lower than that seen with wildtype DAT.

DAT 615C acts dominantly via generation of local negative charge to disrupt AMPH actions

The ADHD subject with whom we initiated our studies is heterozygous for the R615C variant, suggesting that if the variant is a significant risk determinant for the disorder, it likely acts dominantly to alter DAT function. One mechanism by which dominance could be established is from an ability of the DAT R615C variant to preclude association of molecules needed for normal DAT trafficking and function, possibly as a consequence of the transporter's ability to dimerize (Sorkina et al., 2003, Torres et al., 2003). To explore this idea, we synthesized peptides that comprise the last C-terminal 24 amino acids of either DAT 615R or 615C attached to the membrane permeable TAT sequence (Schwarze et al., 1999). Incubation of DAT 615R cells with the TAT-C24^{615R} peptide failed to impact AMPH-mediated downregulation of DA uptake (Fig. 7A). However, incubations of these cells with the TAT-C24^{615C} peptide eliminated the effects of AMPH on the wildtype transporter (Fig. 7A). Addition of either TAT-C24^{615R} or TAT-C24^{615C} peptide (or no peptide) produced no effects on either basal or AMPH-modulated DA transport of DAT 615C cells (Fig. 7B). These findings suggest that rather than attracting molecules that can drive DAT 615C out of GM1 and flotillin-1 containing membrane microdomains, the 615C-substituted C-terminus may preclude interactions needed for successful residency in these compartments.

Next we sought to determine whether the 615C substitution per se perturbs DAT regulation, or whether the loss of Arg residue at this position confers AMPH insensitivity. Following site-directed mutagenesis of the wildtype DAT C-terminus at residue 615, we found that cells transfected with DAT 615A presented a pattern of AMPH regulation indistinguishable from those of DAT 615R (Fig. 7C), indicating that Cys addition versus Arg loss determines AMPH insensitivity. Cytoplasmic Cys residues can be modified by palmitoylation or nitrosylation (Nagahara et al., 2009), modifications that have both been suggested to occur with catecholamine transporters (Kaye et al., 2000, Foster and Vaughan, 2011). However, we detected no differences in palmitoylation between wildtype DAT and the R615C variant, and NOS inhibition did not restore AMPH regulation (data not shown). Cys residues also participate in disulphide bond formation, though this seems unlikely given the reducing environment of the cytosol where the DAT C-terminus resides. Cytoplasmic Cys residues can form acidic thiolates (Nagahara et al., 2009) and as such could confer a charge inversion compared to the wildtype 615R residue. Therefore, we asked whether DAT 615E would also confer insensitivity to AMPH. Indeed, DAT 615E displayed no reductions in DA uptake in response to AMPH treatment (Fig. 7C). Since the mutants 615K, 615A, 615Q, and 615S all respond to AMPH (Fig. 7C), we suggest that a negative thiolate arising from Cys substitution at the 615 position may be responsible for the shift of the DAT R615C variant to AMPH insensitivity.

The Arg residue at 615 of wildtype DAT forms a canonical phosphorylation site for multiple kinases with Thr 613 (Amanchy et al., 2007). However, since the R615A substitution is still AMPH-sensitive, phosphorylation at this site is not required for the psychostimulant's impact on DAT regulation. Consistent with this finding, cells transfected with the T613A mutant retained AMPH sensitivity (Fig. 7D). Moreover, cells transfected with a T613E mutant on the wildtype 615R background to mimic the charge that would be induced by Thr613 phosphorylation lost AMPH sensitivity (Fig. 7D). These findings suggest that Thr613 may need to remain dephosphorylated to sustain psychostimulant (and PKC)

regulation and that a nearby 615C thiol/thiolate may sufficiently mimic the structure or negative charge of phosphorylated Thr613 to preclude DAT regulation by AMPH.

DISCUSSION

ADHD is the most commonly diagnosed disorder of childhood (Smith et al., 2009) and multiple lines of evidence suggest that alterations in DA signaling, including changes in DAT expression or function (Mazei-Robison et al., 2005), can contribute to both cognitive and hyperactive traits of this disorder. In a meta-analysis of association studies examining DAT polymorphisms in ADHD, (Gizer et al., 2009) concluded that although replicable associations are evident, the *SLC6A3* locus is likely to harbor multiple functional variants whose variable influence across families can account for differences in effect sizes detected across studies. To date, however, the majority of genetic studies implicating DAT gene variation with ADHD, or the efficacy of ADHD medications, derive from analysis of a variable number tandem repeat (VNTR) in the 3′-untranslated region. As the functional impact of this VNTR remains ill defined (Winsberg and Comings, 1999, Kirley et al., 2003), aligning these studies with specific alterations in DA signaling is difficult. Rather than focus on common DAT variation of uncertain function, we sought insights into the DA contributions to ADHD via a search for highly penetrant, DAT coding variants. Studies of rare, heritable forms of Alzheimer's disease (Lemere et al., 1996) and Parkinson's disease (Groen et al., 2004) provide two cogent examples of how the elucidation of rare gene variation can lead to novel pathophysiological concepts. Moreover, intensive study of rare variants is justified as such studies can help define broader networks that may elucidate a common underlying pathophysiology.

Recently, we described properties of the DAT coding variant, A559V, identified in two male siblings with ADHD (Mazei-Robison et al., 2005). We found A559V displays increased DAT channel activity and spontaneous, nonvesicular DA release that can be greatly enhanced by membrane depolarization (Mazei-Robison et al., 2008, Bowton et al., 2010). Moreover, spontaneous DA efflux can be attenuated by the ADHD therapeutic AMPH. Here, we describe a second, rare, ADHD-associated DAT coding variant, R615C, where substitution establishes profound basal and regulatory alterations. Although the pedigree harboring the R615C variant is small, with only a single affected carrier, the regulatory disruption we report provides further evidence that changes in DAT-dependent DA signaling contributes to risk for ADHD. Studies with knock-in mice that harbor the R615C variant, similar to those underway in our lab involving the A559V variant (Mergy M.A. and Blakely R.D., Unpublished observations) should allow us to assess which of the multiple *in vitro* alterations in trafficking and regulation we have identified occurs *in vivo*, and how these or other changes impact synaptic DA inactivation.

Multiple elements of DAT's cytoplasmic N- and C-termini have been implicated in basal and regulated control of DAT surface expression, stability and activity. Whereas the DAT N-terminus has been the focus of much research investigating AMPH-induced DA efflux (Khoshbouei et al., 2004b, Fog et al., 2006, Binda et al., 2008), Holton et al., (2005) have proposed that sequences in the C-terminus (residues 587–596) influence basal and PKC-modulated transporter trafficking. The distal C-terminus (residues 618–620) bears a type II PDZ domain interaction motif that has been shown to dictate interactions of the transporter with the PDZ domain protein, PICK1, and possibly enhance DAT surface expression (Torres et al., 2001). Interestingly, Bjerggaard et al., (2004) found that substitution of AAA for the RHW sequence immediately upstream of the PDZ recognition motif leads to ER retention, but preserves the ability of mutant DAT to bind PICK1. The R615C mutation lies in the RHW sequence, and thus an effect on ER/Golgi export may contribute to the transporter's reduced surface expression and DA transport V_{max}.

As previously reported, we found AMPH treatments produce net transporter endocytosis (Saunders et al., 2000, Kahlig et al., 2004, Boudanova et al., 2008a). Activation of PKC isoforms with β-PMA also induces net transporter internalization (Miranda et al., 2007, Boudanova et al., 2008b, Cremona et al., 2011), an effect proposed to be mediated by DAT C-terminal sequences (Holton et al., 2005). Remarkably, we found that the R615C variant demonstrates complete resistance to the trafficking effects of both AMPH and PKC activation. These findings led us to monitor the kinetics of DAT 615C basal and regulated surface trafficking. We found that DAT 615C displays a significantly accelerated rate of both endocytosis and recycling as compared to wildtype DAT. In our cells, treatment with AMPH accelerates the endocytic rates of wildtype DATs, with no detectible change in transporter recycling. Thus, it seems likely that DAT 615C lacks the dynamic range needed to display regulated endo/exocytosis due its high rate of constitutive trafficking.

DAT proteins have been found to reside within cholesterol and GM1 ganglioside-enriched membrane microdomains often referred to as “lipid or membrane rafts” (Sandvig and van Deurs, 2000, Adkins et al., 2007, Foster et al., 2008), and to associate with the raft-associated protein flotillin-1 (Cremona et al., 2011). Also, DATs localized to CTxB-labeled membrane microdomains demonstrate restricted mobility and can be mobilized by membrane cholesterol extraction (Adkins et al., 2007). We found a reduced colocalization of DAT 615C with CTxB-labeled membranes as well as a reduced association of the membrane raft-associated protein flotillin-1. Since quantitation of our co-immunoprecipitation data was normalized for total DAT protein, the reduced flotillin-1 association of the R615C variant may reflect, at least in part, the reduced surface expression of the transporter. However, at present we do not know whether DAT and flotillin-1 have constitutive or dynamic interactions during normal transporter recycling. In the context of our immunofluorescence findings of a surface redistribution of R615C between GM1+ and GM1- compartments, we should also consider that redistribution on the surface might result in targeting DAT to a compartment where opportunities for flotillin-1 interactions are lost. Cremona et al. (2011) provided evidence that interactions with flotillin-1 are required for both PKC-dependent DAT trafficking and AMPH-induced DA efflux. Consistent with these findings, we observed a loss of PKC-induced transporter trafficking with DAT 615C, though AMPH-induced DA efflux was maintained. These findings indicate that DAT/flotillin-1 associations support, but may not be necessary, for AMPH-triggered DA efflux. Since CaMKII associates with DAT through C-terminal sequences that overlay the R615 residue and is critical for AMPH-triggered DA efflux (Fog et al., 2006), the constitutively elevated DAT/CaMKII association may compensate for the loss of flotillin-1 associations, placing mutant transporters in a more DA efflux-competent state. Alternatively, since DAT responds rapidly to AMPH action via increased surface expression (Furman et al., 2009), the R615C substitution may also enhance DAT levels transiently in response to AMPH, during the period of DA efflux measurements. Regardless, these findings raise the possibility that flotillin-1 and CaMKII interactions may be exclusive, with their exchange being a key feature of dynamic DAT regulation. Recently, a Ras-like GTPase, Rin, was shown to associate with DAT C-terminus in membrane rafts and regulate PKC-mediated DAT downregulation (Navaroli et al., 2011). Possibly, the mislocalization and regulatory perturbations we observe with DAT 615C may derive from altered Rin associations, but this issue requires further studies.

As we further explored the role of CaMKII in the insensitivity of the R615C variant to AMPH-induced internalization, we discovered a capacity for the kinase to support a trafficking-independent mode of transporter functional regulation. Specifically, CaMKII activity appears to maintain basal activity of DAT 615C when transporters are localized away from flotillin-1 rich membrane microdomains. Possibly, wildtype DAT residence in membrane microdomains may interfere with the activity of CaMKII, providing a mechanism

whereby physiological stimuli could produce enhanced DAT activity, possibly during states of high DA release. Both norepinephrine and serotonin transporters exhibit similar states of trafficking-independent catalytic regulation (Apparsundaram et al., 2001, Steiner et al., 2008).

Studies examining the physical requirements for AMPH regulation of wildtype DAT in relation to the R615C variant provide key insights into mechanisms supporting transporter regulation. Using TAT-C24^{615R} and TAT-C24^{615C} peptides, we demonstrated that the mutant C-terminus acts dominantly to eliminate AMPH actions on wildtype DAT. These findings are important given the carrier status of our ADHD proband from which the R615C variant was identified. They also indicate that the R615C may compete in the hemizygous state with the wild-type DAT C-terminus for key interactions needed for AMPH-induced transporter regulation. Additionally, we found that whereas 615C precludes AMPH-induced transporter downregulation, Ala, Lys, Gln, and Ser substitutions for R615 fail to perturb regulation. In further pursuit of the structural basis for the 615C effect, we found that 615E recapitulated the impact of 615C, suggesting that the generation of negative charge in the distal C-terminus may play a role in disrupting transporter regulation. Cys residues can exist as thiolates and thereby create a local negative charge (Nagahara et al., 2009). Whereas the pKa of a free Cys thiol is estimated at ~8, leaving the Cys side chain of 615C largely protonated, the pKa of proteinaceous Cys residues is known to be quite sensitive to its local environment, where the thiolate anion can be stabilized by surrounding residues (Netto et al., 2007).

Since R615 forms a phosphorylation site motif with T613, we considered the possibility that 615C gains its capacity to disrupt regulation by interfering with T613 phosphorylation. However, we found that a T613E mutation, created to produce the negative charge associated with Thr phosphorylation, recapitulates the behavior of 615C. These findings suggest that *dephosphorylation* of T613 may be a critical step in sorting DAT into regulated versus constitutive endocytic pathways. Further studies are needed to determine whether, and under what conditions, kinases and phosphatases may target this residue, either constitutively or as part of a rapid, regulatory mechanism, or whether other mechanisms, such as charge-dependent protein associations, impart sorting decisions.

In toto, our findings lead us to propose a two-compartment model that organizes our findings (Figure 8). DAT exists at the cell surface in GM1/flotillin-1 enriched microdomains that restrict transporter lateral mobility and provide for regulated trafficking. Alternatively, the transporter can reside in membrane depleted of these raft components and here traffics largely via constitutive endocytosis and rapid recycling. Decisions dictating the localization and trafficking of DAT are dependent on sequences in the distal C-terminus of DAT, which we suspect involves phosphorylation/dephosphorylation reactions at T613. Our model has parallels with the differential trafficking of insulin-responsive (GLUT4) and nonresponsive (GLUT1) glucose transporters. GLUT4 and GLUT1 equivalently support glucose uptake, but GLUT4 traffics through a limited capacity, regulated pathway whereas, GLUT1, traffics in the same cells through higher-capacity, constitutive mechanisms (Zorzano et al., 1997). Wildtype DAT has the capacity to occupy either a regulated or constitutive pathway, but in our model systems is biased normally toward GM1/flotillin-1 enriched domains. As shown by our studies with the DAT^{615C} peptide, the DAT-C terminus can play a dominant role in the transporter's capacity for regulated trafficking. The DNA encoding DAT 615 and the other mutants generated in this study, as well as the DAT^{615C} peptide should be useful in further elucidating the mechanisms by which DAT sorts between constitutive and regulated trafficking pathways. Although the R615C variant is rare, our findings suggest that a more intensive analysis of proteins that influence DAT localization and function within membrane microdomains may provide important insights for idiopathic ADHD.

Acknowledgments

This research was supported by National Institute of Health (NIH) predoctoral fellowships MH067472 (M.S.M.-R) MH090738 (M.M.) MH064913 (E.B.), and a National Science Foundation (NSF) fellowship DGE0909667 (P.J.H.). R.D.B. was supported by NIH award HL56693. A.G. was supported by NIH awards DA013975 and DA014684. We thank Mark Stein (University of Illinois, Chicago) and Irwin Waldman (Emory University) for contribution of DNAs from ADHD subjects for this study. We thank Chris Svitek, Jane Wright, and Angela Steele for laboratory oversight and technical assistance. D.S. thanks the Vanderbilt Brain Institute for graduate training support and Roger Colbran for critical review of the manuscript.

References

Adkins EM, Samuvel DJ, Fog JU, Eriksen J, Jayanthi LD, Vaegter CB, Ramamoorthy S, Gether U. Membrane mobility and microdomain association of the dopamine transporter studied with fluorescence correlation spectroscopy and fluorescence recovery after photobleaching. Biochemistry. 2007; 46:10484–10497. [PubMed: 17711354]

Amanchy R, Periaswamy B, Mathivanan S, Reddy R, Tattikota SG, Pandey A. A curated compendium of phosphorylation motifs. Nat Biotechnol. 2007; 25:285–286. [PubMed: 17344875]

Apparsundaram S, Galli A, DeFelice LJ, Hartzell HC, Blakely RD. Acute regulation of norepinephrine transport: I. protein kinase C-linked muscarinic receptors influence transport capacity and transporter density in SK-N-SH cells. J Pharmacol Exp Ther. 1998; 287:733–743. [PubMed: 9808704]

Apparsundaram S, Sung U, Price RD, Blakely RD. Trafficking-dependent and -independent pathways of neurotransmitter transporter regulation differentially involving p38 mitogen-activated protein kinase revealed in studies of insulin modulation of norepinephrine transport in SK-N-SH cells. J Pharmacol Exp Ther. 2001; 299:666–677. [PubMed: 11602680]

Baucum AJ 2nd, Jalan-Sakrikar N, Jiao Y, Gustin RM, Carmody LC, Tabb DL, Ham AJ, Colbran RJ. Identification and validation of novel spinophilin-associated proteins in rodent striatum using an enhanced ex vivo shotgun proteomics approach. Mol Cell Proteomics. 2010; 9:1243–1259. [PubMed: 20124353]

Bellgrove MA, Johnson KA, Barry E, Mulligan A, Hawi Z, Gill M, Robertson I, Chambers CD. Dopaminergic haplotype as a predictor of spatial inattention in children with attention-deficit/hyperactivity disorder. Arch Gen Psychiatry. 2009; 66:1135–1142. [PubMed: 19805704]

Binda F, Dipace C, Bowton E, Robertson SD, Lute BJ, Fog JU, Zhang M, Sen N, Colbran RJ, Gnegy ME, Gether U, Javitch JA, Erreger K, Galli A. Syntaxin 1A interaction with the dopamine transporter promotes amphetamine-induced dopamine efflux. Molecular pharmacology. 2008; 74:1101–1108. [PubMed: 18617632]

Bjerggaard C, Fog JU, Hastrup H, Madsen K, Loland CJ, Javitch JA, Gether U. Surface targeting of the dopamine transporter involves discrete epitopes in the distal C terminus but does not require canonical PDZ domain interactions. The Journal of neuroscience : the official journal of the Society for Neuroscience. 2004; 24:7024–7036. [PubMed: 15295038]

Bobb AJ, Castellanos FX, Addington AM, Rapoport JL. Molecular genetic studies of ADHD: 1991 to 2004. Am J Med Genet B Neuropsychiatr Genet. 2005; 132B:109–125. [PubMed: 15700344]

Boudanova E, Navaroli DM, Melikian HE. Amphetamine-induced decreases in dopamine transporter surface expression are protein kinase C-independent. Neuropharmacology. 2008a; 54:605–612. [PubMed: 18164041]

Boudanova E, Navaroli DM, Stevens Z, Melikian HE. Dopamine transporter endocytic determinants: carboxy terminal residues critical for basal and PKC-stimulated internalization. Mol Cell Neurosci. 2008b; 39:211–217. [PubMed: 18638559]

Bowton E, Saunders C, Erreger K, Sakrikar D, Matthies HJ, Sen N, Jessen T, Colbran RJ, Caron MG, Javitch JA, Blakely RD, Galli A. Dysregulation of dopamine transporters via dopamine D2 autoreceptors triggers anomalous dopamine efflux associated with attention-deficit hyperactivity disorder. The Journal of neuroscience : the official journal of the Society for Neuroscience. 2010; 30:6048–6057. [PubMed: 20427663]

Carlsson A. Perspectives on the discovery of central monoaminergic neurotransmission. Annu Rev Neurosci. 1987; 10:19–40. [PubMed: 3032064]

Chase TN, Oh JD, Blanchet PJ. Neostriatal mechanisms in Parkinson's disease. Neurology. 1998; 51:S30–35. [PubMed: 9711978]

Chen R, Furman CA, Gnegy ME. Dopamine transporter trafficking: rapid response on demand. Future Neurol. 2010; 5:123. [PubMed: 20174452]

Cremona ML, Matthies HJ, Pau K, Bowton E, Speed N, Lute BJ, Anderson M, Sen N, Robertson SD, Vaughan RA, Rothman JE, Galli A, Javitch JA, Yamamoto A. Flotillin-1 is essential for PKC-triggered endocytosis and membrane microdomain localization of DAT. Nat Neurosci. 2011; 14:469–477. [PubMed: 21399631]

Deken SL, Wang D, Quick MW. Plasma membrane GABA transporters reside on distinct vesicles and undergo rapid regulated recycling. The Journal of neuroscience : the official journal of the Society for Neuroscience. 2003; 23:1563–1568. [PubMed: 12629157]

Fog JU, Khoshbouei H, Holy M, Owens WA, Vaegter CB, Sen N, Nikandrova Y, Bowton E, McMahon DG, Colbran RJ, Daws LC, Sitte HH, Javitch JA, Galli A, Gether U. Calmodulin kinase II interacts with the dopamine transporter C terminus to regulate amphetamine-induced reverse transport. Neuron. 2006; 51:417–429. [PubMed: 16908408]

Foster JD, Adkins SD, Lever JR, Vaughan RA. Phorbol ester induced trafficking-independent regulation and enhanced phosphorylation of the dopamine transporter associated with membrane rafts and cholesterol. J Neurochem. 2008; 105:1683–1699. [PubMed: 18248623]

Foster JD, Vaughan RA. Palmitoylation controls dopamine transporter kinetics, degradation, and protein kinase C-dependent regulation. The Journal of biological chemistry. 2011; 286:5175–5186. [PubMed: 21118819]

Furman CA, Chen R, Guptaroy B, Zhang M, Holz RW, Gnegy M. Dopamine and amphetamine rapidly increase dopamine transporter trafficking to the surface: live-cell imaging using total internal reflection fluorescence microscopy. The Journal of neuroscience : the official journal of the Society for Neuroscience. 2009; 29:3328–3336. [PubMed: 19279270]

Gill M, Daly G, Heron S, Hawi Z, Fitzgerald M. Confirmation of association between attention deficit hyperactivity disorder and a dopamine transporter polymorphism. Mol Psychiatry. 1997; 2:311–313. [PubMed: 9246671]

Giros B, Jaber M, Jones SR, Wightman RM, Caron MG. Hyperlocomotion and indifference to cocaine and amphetamine in mice lacking the dopamine transporter. Nature. 1996; 379:606–612. [PubMed: 8628395]

Gizer IR, Ficks C, Waldman ID. Candidate gene studies of ADHD: a meta-analytic review. Hum Genet. 2009; 126:51–90. [PubMed: 19506906]

Gnegy ME, Khoshbouei H, Berg KA, Javitch JA, Clarke WP, Zhang M, Galli A. Intracellular Ca2+ regulates amphetamine-induced dopamine efflux and currents mediated by the human dopamine transporter. Molecular pharmacology. 2004; 66:137–143. [PubMed: 15213305]

Groen JL, Kawarai T, Toulina A, Rivoiro C, Salehi-Rad S, Sato C, Morgan A, Liang Y, Postuma RB, St George-Hyslop P, Lang AE, Rogaeva E. Genetic association study of PINK1 coding polymorphisms in Parkinson's disease. Neurosci Lett. 2004; 372:226–229. [PubMed: 15542245]

Holton KL, Loder MK, Melikian HE. Nonclassical, distinct endocytic signals dictate constitutive and PKC-regulated neurotransmitter transporter internalization. Nat Neurosci. 2005; 8:881–888. [PubMed: 15924135]

Hong WC, Amara SG. Membrane cholesterol modulates the outward facing conformation of the dopamine transporter and alters cocaine binding. The Journal of biological chemistry. 2010; 285:32616–32626. [PubMed: 20688912]

Kahlig KM, Javitch JA, Galli A. Amphetamine regulation of dopamine transport. Combined measurements of transporter currents and transporter imaging support the endocytosis of an active carrier. The Journal of biological chemistry. 2004; 279:8966–8975. [PubMed: 14699142]

Kahlig KM, Lute BJ, Wei Y, Loland CJ, Gether U, Javitch JA, Galli A. Regulation of dopamine transporter trafficking by intracellular amphetamine. Molecular pharmacology. 2006; 70:542–548. [PubMed: 16684900]

Kaye DM, Gruskin S, Smith AI, Esler MD. Nitric oxide mediated modulation of norepinephrine transport: identification of a potential target for S-nitrosylation. Br J Pharmacol. 2000; 130:1060–1064. [PubMed: 10882390]

Khoshbouei H, Sen N, Guptaroy B, Johnson L, Lund D, Gnegy ME, Galli A, Javitch JA. N-terminal phosphorylation of the dopamine transporter is required for amphetamine-induced efflux. PLoS Biol. 2004a; 2:E78. [PubMed: 15024426]

Khoshbouei H, Sen N, Guptaroy B, Johnson L, Lund D, Gnegy ME, Galli A, Javitch JA. N-terminal phosphorylation of the dopamine transporter is required for amphetamine-induced efflux. PLoS biology. 2004b; 2:E78. [PubMed: 15024426]

Khoshbouei H, Wang H, Lechleiter JD, Javitch JA, Galli A. Amphetamine-induced dopamine efflux. A voltage-sensitive and intracellular Na+-dependent mechanism. The Journal of biological chemistry. 2003; 278:12070–12077. [PubMed: 12556446]

Kirley A, Lowe N, Hawi Z, Mullins C, Daly G, Waldman I, McCarron M, O'Donnell D, Fitzgerald M, Gill M. Association of the 480 bp DAT1 allele with methylphenidate response in a sample of Irish children with ADHD. Am J Med Genet B Neuropsychiatr Genet. 2003; 121B:50–54. [PubMed: 12898575]

Kurian MA, Zhen J, Cheng SY, Li Y, Mordekar SR, Jardine P, Morgan NV, Meyer E, Tee L, Pasha S, Wassmer E, Heales SJ, Gissen P, Reith ME, Maher ER. Homozygous loss-of-function mutations in the gene encoding the dopamine transporter are associated with infantile parkinsonism-dystonia. J Clin Invest. 2009; 119:1595–1603. [PubMed: 19478460]

Lemere CA, Lopera F, Kosik KS, Lendon CL, Ossa J, Saido TC, Yamaguchi H, Ruiz A, Martinez A, Madrigal L, Hincapie L, Arango JC, Anthony DC, Koo EH, Goate AM, Selkoe DJ. The E280A presenilin 1 Alzheimer mutation produces increased A beta 42 deposition and severe cerebellar pathology. Nat Med. 1996; 2:1146–1150. [PubMed: 8837617]

Li Q, Liu Z, Monroe H, Culiat CT. Integrated platform for detection of DNA sequence variants using capillary array electrophoresis. Electrophoresis. 2002; 23:1499–1511. [PubMed: 12116161]

Loder MK, Melikian HE. The dopamine transporter constitutively internalizes and recycles in a protein kinase C-regulated manner in stably transfected PC12 cell lines. The Journal of biological chemistry. 2003; 278:22168–22174. [PubMed: 12682063]

Mazei-Robison MS, Blakely RD. Expression studies of naturally occurring human dopamine transporter variants identifies a novel state of transporter inactivation associated with Val382Ala. Neuropharmacology. 2005; 49:737–749. [PubMed: 16212992]

Mazei-Robison MS, Bowton E, Holy M, Schmudermaier M, Freissmuth M, Sitte HH, Galli A, Blakely RD. Anomalous dopamine release associated with a human dopamine transporter coding variant. The Journal of neuroscience : the official journal of the Society for Neuroscience. 2008; 28:7040–7046. [PubMed: 18614672]

Mazei-Robison MS, Couch RS, Shelton RC, Stein MA, Blakely RD. Sequence variation in the human dopamine transporter gene in children with attention deficit hyperactivity disorder. Neuropharmacology. 2005; 49:724–736. [PubMed: 16171832]

Miranda M, Dionne KR, Sorkina T, Sorkin A. Three ubiquitin conjugation sites in the amino terminus of the dopamine transporter mediate protein kinase C-dependent endocytosis of the transporter. Mol Biol Cell. 2007; 18:313–323. [PubMed: 17079728]

Nagahara N, Matsumura T, Okamoto R, Kajihara Y. Protein cysteine modifications: (1) medical chemistry for proteomics. Curr Med Chem. 2009; 16:4419–4444. [PubMed: 19835564]

Navaroli DM, Stevens ZH, Uzelac Z, Gabriel L, King MJ, Lifshitz LM, Sitte HH, Melikian HE. The plasma membrane-associated GTPase rin interacts with the dopamine transporter and is required for protein kinase C-regulated dopamine transporter trafficking. The Journal of neuroscience : the official journal of the Society for Neuroscience. 2011; 31:13758–13770. [PubMed: 21957239]

Netto LE, de Oliveira MA, Monteiro G, Demasi AP, Cussiol JR, Discola KF, Demasi M, Silva GM, Alves SV, Faria VG, Horta BB. Reactive cysteine in proteins: protein folding, antioxidant defense, redox signaling and more. Comp Biochem Physiol C Toxicol Pharmacol. 2007; 146:180–193. [PubMed: 17045551]

Qi Y, Wang JKT, McMillian M, Chikaraishi DM. Characterization of a CNS cell line, CAD, in which morphological differentiation is initiated by serum deprivation. The Journal of Neuroscience. 1997; 17(4):1217–1225. [PubMed: 9006967]

Qian Q, Wang Y, Zhou R, Li J, Wang B, Glatt S, Faraone SV. Family-based and case- control association studies of catechol-O-methyltransferase in attention deficit hyperactivity disorder

suggest genetic sexual dimorphism. Am J Med Genet B Neuropsychiatr Genet. 2003; 118B:103–109. [PubMed: 12627475]

Ritz MC, Lamb RJ, Goldberg SR, Kuhar MJ. Cocaine receptors on dopamine transporters are related to self-administration of cocaine. Science. 1987; 237:1219–1223. [PubMed: 2820058]

Robbins TW. Dopamine and cognition. Curr Opin Neurol. 2003; 16(Suppl 2):S1–2. [PubMed: 15129843]

Sandvig K, van Deurs B. Entry of ricin and Shiga toxin into cells: molecular mechanisms and medical perspectives. Embo J. 2000; 19:5943–5950. [PubMed: 11080141]

Sauer B. Site-specific recombination: developments and applications. Curr Opin Biotechnol. 1994; 5:521–527. [PubMed: 7765467]

Saunders C, Ferrer JV, Shi L, Chen J, Merrill G, Lamb ME, Leeb-Lundberg LM, Carvelli L, Javitch JA, Galli A. Amphetamine-induced loss of human dopamine transporter activity: an internalization-dependent and cocaine-sensitive mechanism. Proc Natl Acad Sci U S A. 2000; 97:6850–6855. [PubMed: 10823899]

Schwarze SR, Ho A, Vocero-Akbani A, Dowdy SF. In vivo protein transduction: delivery of a biologically active protein into the mouse. Science. 1999; 285:1569–1572. [PubMed: 10477521]

Simons K, Ikonen E. Functional rafts in cell membranes. Nature. 1997; 387:569–572. [PubMed: 9177342]

Smith AK, Mick E, Faraone SV. Advances in genetic studies of attention-deficit/hyperactivity disorder. Curr Psychiatry Rep. 2009; 11:143–148. [PubMed: 19302768]

Sorkina T, Doolen S, Galperin E, Zahniser NR, Sorkin A. Oligomerization of dopamine transporters visualized in living cells by fluorescence resonance energy transfer microscopy. The Journal of biological chemistry. 2003; 278:28274–28283. [PubMed: 12746456]

Sorkina T, Miranda M, Dionne KR, Hoover BR, Zahniser NR, Sorkin A. RNA interference screen reveals an essential role of Nedd4-2 in dopamine transporter ubiquitination and endocytosis. The Journal of neuroscience : the official journal of the Society for Neuroscience. 2006; 26:8195–8205. [PubMed: 16885233]

Steiner JA, Carneiro AM, Blakely RD. Going with the flow: trafficking-dependent and -independent regulation of serotonin transport. Traffic. 2008; 9:1393–1402. [PubMed: 18445122]

Steiner JA, Carneiro AM, Wright J, Matthies HJ, Prasad HC, Nicki CK, Dostmann WR, Buchanan CC, Corbin JD, Francis SH, Blakely RD. cGMP-dependent protein kinase Ialpha associates with the antidepressant-sensitive serotonin transporter and dictates rapid modulation of serotonin uptake. Mol Brain. 2009; 2:26. [PubMed: 19656393]

Sulzer D, Sonders MS, Poulsen NW, Galli A. Mechanisms of neurotransmitter release by amphetamines: a review. Prog Neurobiol. 2005; 75:406–433. [PubMed: 15955613]

Swanson JM, Kinsbourne M, Nigg J, Lanphear B, Stefanatos GA, Volkow N, Taylor E, Casey BJ, Castellanos FX, Wadhwa PD. Etiologic subtypes of attention-deficit/hyperactivity disorder: brain imaging, molecular genetic and environmental factors and the dopamine hypothesis. Neuropsychol Rev. 2007; 17:39–59. [PubMed: 17318414]

Torres GE, Carneiro A, Seamans K, Fiorentini C, Sweeney A, Yao WD, Caron MG. Oligomerization and trafficking of the human dopamine transporter. Mutational analysis identifies critical domains important for the functional expression of the transporter. The Journal of biological chemistry. 2003; 278:2731–2739. [PubMed: 12429746]

Torres GE, Yao WD, Mohn AR, Quan H, Kim KM, Levey AI, Staudinger J, Caron MG. Functional interaction between monoamine plasma membrane transporters and the synaptic PDZ domain-containing protein PICK1. Neuron. 2001; 30:121–134. [PubMed: 11343649]

Wei Y, Williams JM, Dipace C, Sung U, Javitch JA, Galli A, Saunders C. Dopamine transporter activity mediates amphetamine-induced inhibition of Akt through a Ca2+/calmodulin-dependent kinase II-dependent mechanism. Mol Pharmacol. 2007; 71:835–842. [PubMed: 17164407]

Winsberg BG, Comings DE. Association of the dopamine transporter gene (DAT1) with poor methylphenidate response. J Am Acad Child Adolesc Psychiatry. 1999; 38:1474–1477. [PubMed: 10596245]

Zorzano A, Sevilla L, Camps M, Becker C, Meyer J, Kammermeier H, Munoz P, Guma A, Testar X, Palacin M, Blasi J, Fischer Y. Regulation of glucose transport, and glucose transporters expression

and trafficking in the heart: studies in cardiac myocytes. Am J Cardiol. 1997; 80:65A–76A. [PubMed: 9205022]

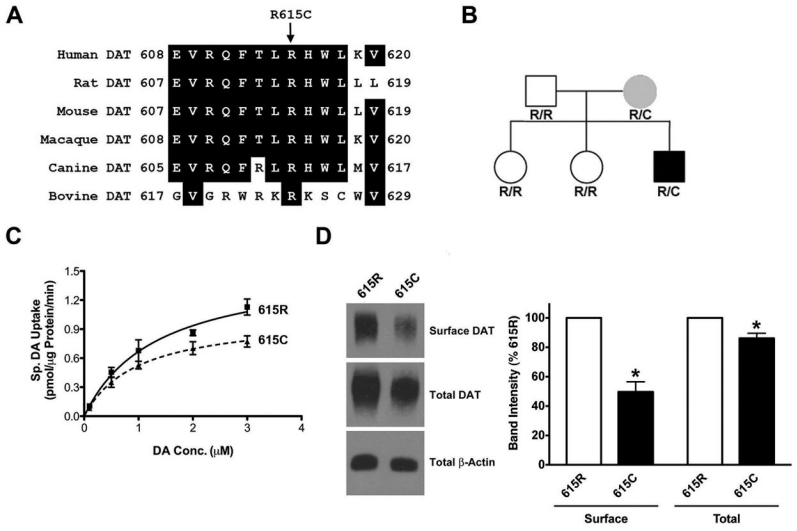

Figure 1. Reduced surface expression and DA transport V_{max} associated with the R615C variant

(A) Sequence alignment showing conservation of arginine 615 across mammalian DATs. **(B)** Pedigree of ADHD proband carrying the R615C variant. The subject (black box) was heterozygous for the R615C-DAT variant. Transmission of the mutant allele occurred from mother (grey circle). Other family members (father and two older sisters) were unaffected. **(C)** DA transport V_{max} and K_m are expressed as pmol/μg protein/min and μM respectively. K_m & V_{max} values are expressed as ± the SEM. A significant decrease in the DA transport V_{max} was observed for DAT 615C without a significant change K_m. **(D)** Left: Representative western blot showing reduction in the surface and total DAT for the R615C variant compared to 615R. Total protein levels of β-actin, an intracellular loading control, were similar for both 615R and 615C. Right: Quantification from six independent experiments indicating significant reduction in the R615C variant compared to 615R surface and total expression. Total protein samples were diluted 5 fold compared to the surface protein fraction to retain signal linearity.

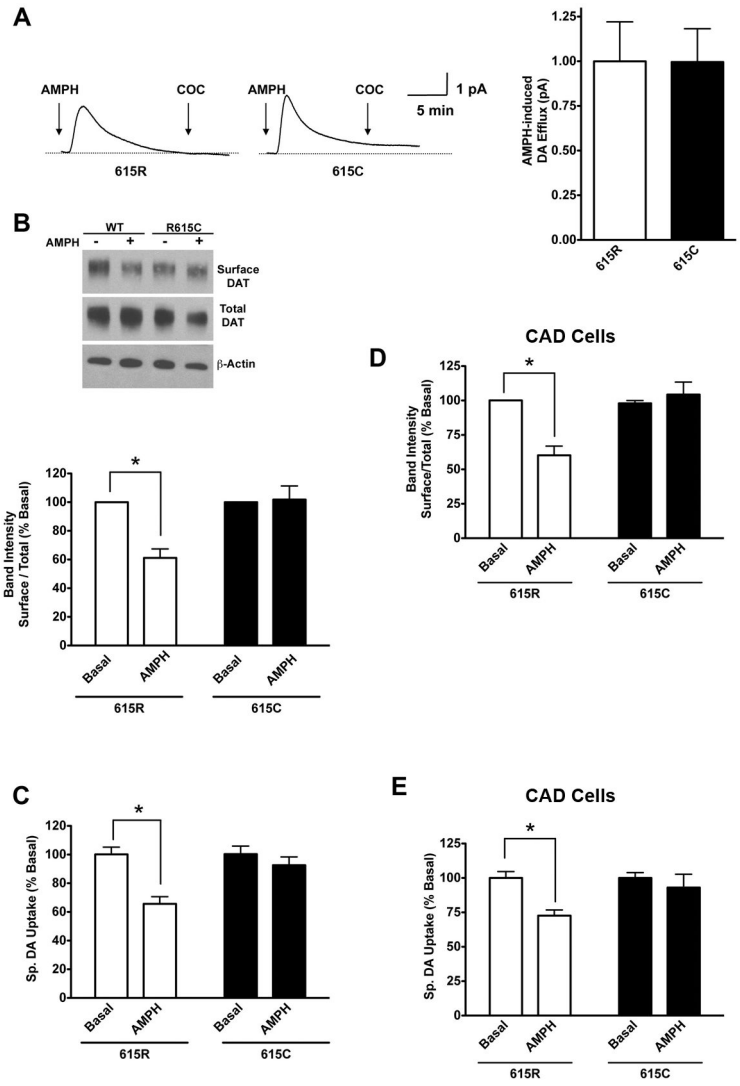

Figure 2. Anomalous modulation of DAT 615C by AMPH

(A) Flp-In 293 stable cells were preloaded with 1 μM DA for 20 min and AMPH-induced DA efflux was measured using carbon fiber amperometry. AMPH-induced DA efflux from DAT 615C was not significantly different than 615R (1.0±0.22 pA for 615R vs. 0.996±0.18 pA for 615C). **(B)** Top: Representative western blot showing surface DAT protein levels after AMPH treatment (10 μM, 30 minutes) for DAT 615C were significantly greater than AMPH treated 615R surface levels. Total β-actin is used as an intracellular loading control. Bottom: Quantification of AMPH-induced decrease in DAT surface levels expressed as surface/total. Data is normalized to basal DAT surface/total expressions as 100%. AMPH treatment caused a significant (62±7%) decrease in the DAT 615R expression while no change was detected in 615C expression (95±8%). Significant differences were calculated using one-way ANOVA followed by Bonferroni's post hoc test. (n=7, $P<0.0001$) **(C)** AMPH-mediated (10 μM, 30 minutes) reduction in the DA transport seen in DAT 615R (white bar; AMPH) is lost for 615C (black bar; AMPH). Basal DA transport levels were normalized to respective cell lines and AMPH-mediated reduction was measured. AMPH caused a significant decrease (66±5 % of basal) in the DA transport of DAT 615R while no significant changes were detected for 615C (93±6 % of basal). Significant differences were calculated using one-way ANOVA followed by Bonferroni's post hoc test. (n=3, $P<0.001$)

(D) Quantification of AMPH-induced decrease in DAT surface levels expressed as surface/total from transiently transfected CAD cells. Data is normalized to basal DAT surface/total expressions as 100%. AMPH treatment caused a significant (63±6%) decrease in the DAT 615R expression while no change was detected in 615C expression (104±9%). Significant differences were calculated using one-way ANOVA followed by Bonferroni's post hoc test. (n=4, $P<0.0001$) **(E)** Transiently transfected, neuronally derived CAD cells display similar loss of AMPH-mediated reduction in DA transport seen in Flp-In HEK stable cells lines. Basal DA transport levels were normalized to respective cell lines and AMPH-mediated reduction was measured. AMPH caused a significant decrease (72±4 % of basal) in the DA transport of DAT 615R while no significant changes were detected for 615C (93±9 % of basal). Significant differences were calculated using one-way ANOVA followed by Bonferroni's post hoc test. (n=4, $P<0.01$)

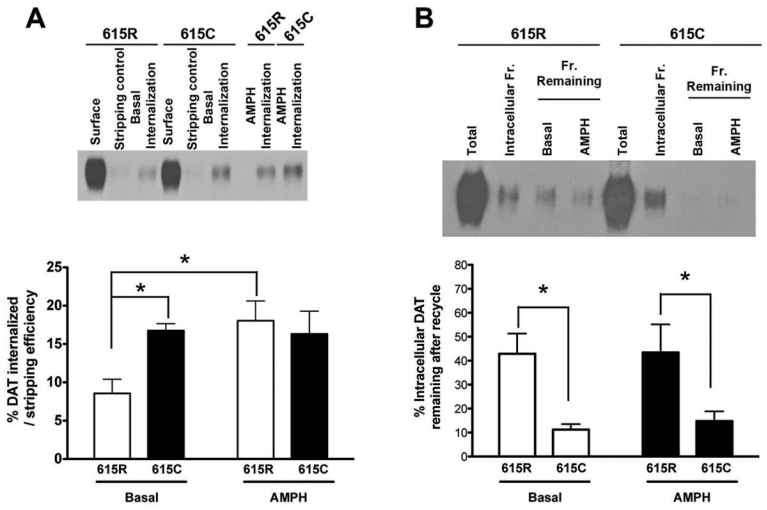

Figure 3. DAT 615C exhibits accelerated rates of constitutive endocytosis and recycling

(A) Top: Representative western blot showing increased basal endocytosis associated with the R615C variant. AMPH treatment (10 μM, 30 minutes) caused significant increase in internalization of DAT 615R without affecting 615C internalization rate. Bottom: Quantification of internalization rates normalized to stripping efficiency. Basal internalization rate of DAT 615C was significantly increased compared to 615R (16.7±0.9% for 615C vs. 8.5±1.8% for 615R; n=3, $P<0.05$, Student's t test). AMPH treatment significantly increased internalization rate of DAT 615R (8.5±1.8% for basal vs. 18±2.6% for AMPH; n=3, $P<0.05$, Student's t test) without affecting the R615C variant (16.7±0.9% for basal vs. 16.3±2.9% for AMPH; n=3, $P>0.05$, Student's t test). **(B)** Top: Representative western blot showing accelerated recycling of R615C variant. AMPH treatment (10 μM, 30 minutes) did not impact the recycling rate for both DAT 615R and 615C. Bottom: Quantification of recycling rate normalized to intracellular DAT fraction. A bigger fraction of DAT still remains intracellularly after constitutive recycling for DAT 615R compared to 615C (42.9±8% for 615R vs. 11.2±2.3% for 615C; n=6, $P<0.005$, Student's t test). AMPH treatment did not alter fractional DAT remaining inside after recycling (basal-42.9±8% vs. AMPH-43.4±11.7% for DAT 615R and basal-11.2±2.3% vs. AMPH-14.8±4.1% for DAT 651C; n=3–6, $P>0.05$, Student's t test).

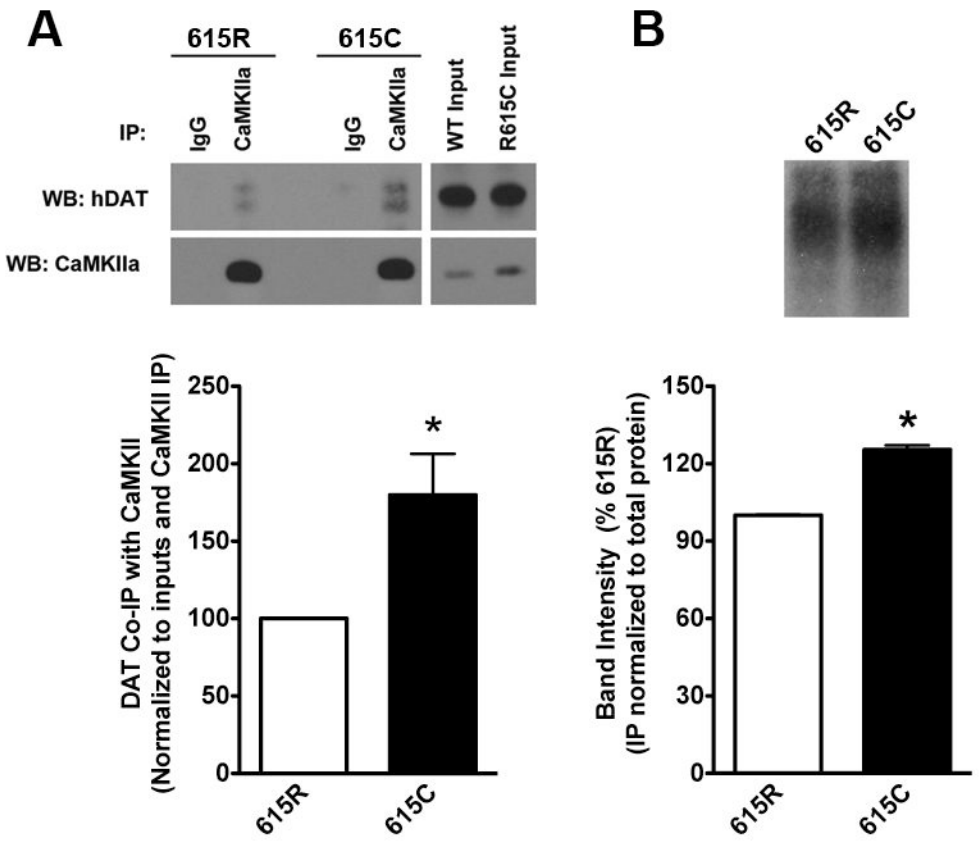

Figure 4. Increased basal CaMKII association and phosphorylation of the R615C variant

(A) Top: Representative western blot showing increased association between DAT 615C and CaMKII compared to 615R. Bottom: Quantification of DAT co-IP with CaMKII normalized to respective inputs. Significantly larger pool of 615C is co-precipitated with CaMKII (179±26 % of 615R; n=3, $P<0.05$, Student's t test). **(B)** Top: Representative autoradiograph indicating increased basal phosphorylation of DAT 615C compared to 615R Bottom: Quantification of DAT bands from the autoradiograph showing significant increase in basal phosphorylation levels of DAT 615C (125±1.6 % of 615R; n=3, $P<0.05$, Student's t test). Equal total protein amounts were used for IP following the metabolic labeling.

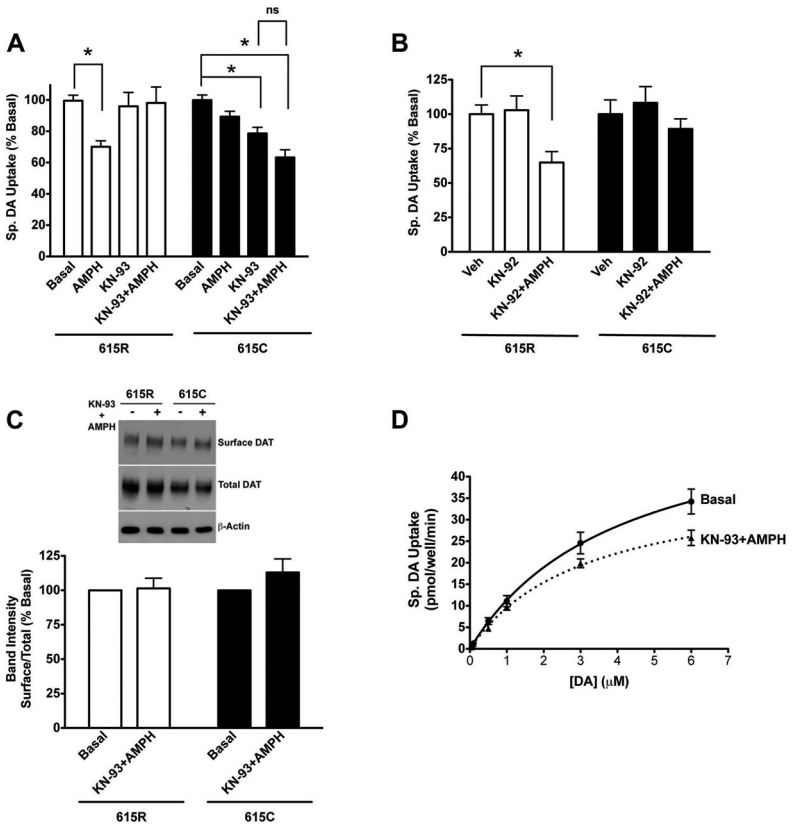

Figure 5. DAT R615C reveals a CAMKII-dependent state of functional inactivation

(A) KN-93 (1 μM, 30 minutes) treatment (black bar, KN-93) caused a significant DA transport reduction in 615C (79±4% of basal) while showing no effect on WT-DAT (white bar, KN-93, 95±9% of basal). Pretreatment with KN-93 before AMPH (10 μM, 30 minutes) addition blocked AMPH-mediated DA transport reduction in DAT 615R (white bars, AMPH (70±4%) vs. KN-93+AMPH (98±10%)) while DAT 615C showed significant reduction upon KN-93+AMPH treatment (black bars, AMPH (89±3%) vs. KN-93+AMPH (63±5%)). The reduction upon KN-93+AMPH treatment was not significantly different from the reduction obtained by treatment with KN-93 alone in the R615C variant (79±4% for KN-93 vs. 63±5% for KN-93+AMPH). Data were normalized to basal DA uptake of respective cell lines. Significant differences were calculated using one-way ANOVA followed by Bonferroni's post hoc test. (n=3–6, $P<0.0001$) **(B)** An inactive analog of KN-93, KN-92, by itself did not affect DA uptake in either DAT 615R (white bar, KN-92; 102±10% of basal) or 615C (black bar, KN-92; 108±12%of basal). Pretreatment with KN-92 (1 μM, 30 minutes) did not block AMPH-mediated (10 μM, 30 minutes) DA transport reduction in DAT 615R (white bar, KN-92+AMPH, 65±8% of basal) and had not effect on 615C (black bar, KN-92+AMPH, 90±7% of basal). Data were normalized to basal DA uptake of respective cell lines. Significant differences were calculated using one-way ANOVA followed by Bonferroni's post hoc test. (n=3, $P<0.05$) **(C)** Top: Representative western blots showing KN-93+AMPH treatment did not cause reduction in DAT surface levels for both DAT 615R and 615C. Bottom: Quantification showing KN-93+AMPH (1 μM KN-93 for 30 minutes followed by 10 μM AMPH for 30 minutes) treatment rescued the reduction in the DAT surface expression of DAT 615R (101±7% of basal) similar to results obtained by DA uptake assays. KN-93+AMPH treatment showed no change (113±10% of basal) in the surface levels of DAT 615C. The differences obtained from the KN-93+AMPH treatment were not statistically significant from their basal correlates assessed by one-way

ANOVA. (n=7, $P>0.05$) **(D)** KN-93+AMPH (1 μM KN-93 for 30 minutes followed by 10 μM AMPH for 30 minutes) treatment resulted in significant reduction in DA transport V_{max} for the R615C variant. DA transport V_{max} and K_m are expressed as pmol/well/min and μM respectively. A significant decrease in the DA transport V_{max} was observed after KN-93+AMPH treatment (65±10, basal vs. 42±3, KN-93+AMPH; n=4, $P<0.05$, Student's t test) without a significant change in K_m (5.4±1.5, basal vs. 3.8±0.6, KN-93+AMPH; n=4, $P>0.05$, Student's t test).

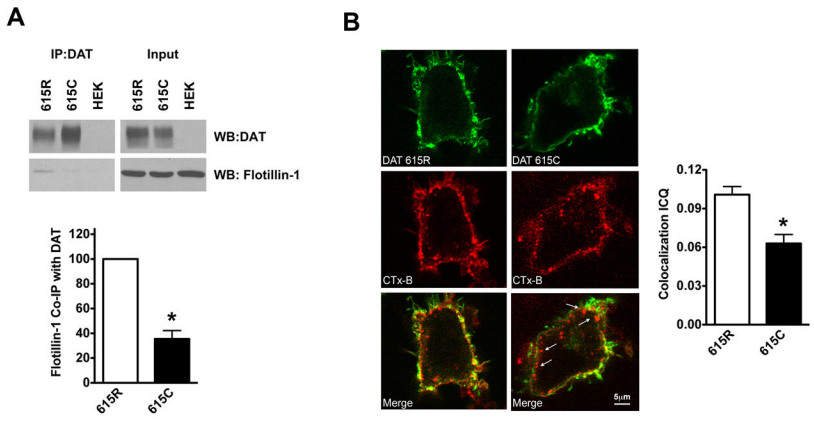

Figure 6. Altered membrane raft microdomain association of the R615C variant

(A) Top: Representative western blot showing reduced association of DAT 615C with flotillin-1. Bottom: Quantification of flotillin-1 co-IP with DAT normalized to respective inputs. DAT 615C displays significantly reduced association with flotillin-1 (33±8 % of 615R; n=5, $P<0.001$, Student's t test). **(B)** Top: HEK 293T cells are transiently transfected with YFP-HA-hDATs (green). Alexa 647 conjugated cholera toxin B is used to mark GM1 ganglioside (red). Representative cells are shown with white arrows indicating lack of DAT association with the raft fraction of R615C variant. Bottom: ICQ analysis is performed to define colocalization of YFP-DAT with CTx-B labeled lipid rafts. Quantification demonstrated that although both 615R and 615C DAT are significantly colocalized with CTx-B, 615C exhibits a significantly reduced ICQ value compared to 615R (615R, 0.1±0.006 vs. 615C, 0.06±0.006; n=22, $P<0.01$, Student's t test).

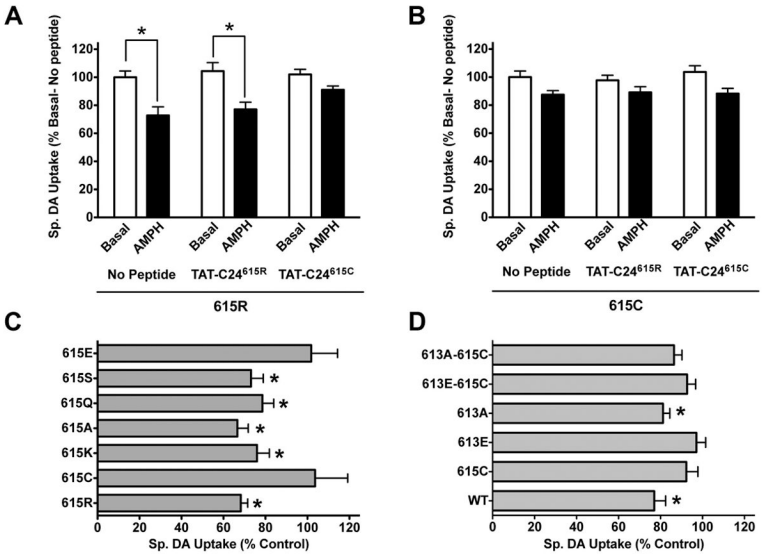

Figure 7. DAT 615C acts dominantly via generation of local negative charge to disrupt AMPH actions

(A, B) Exogenous addition of TAT-C24^{615C} peptide blocks AMPH-mediated reduction in the DA transport for DAT 615R and had no effect on 615C. Addition of either TAT-C24^{615R} or TAT-C24^{615C} peptide (10 μM, 18hrs) did not alter basal DA uptake compared to no peptide control for both DAT 615R and 615C (for DAT 615R, 104±6% with TAT-C24^{615R} and 102±3% with TAT-C24^{615C}; for DAT 615C, 96±3% with TAT-C24^{615R} and 103±4% with TAT-C24^{615C}). Addition of TAT-C24^{615R} peptide or no peptide control produced a significant reduction in DA uptake for DAT 615R upon AMPH (10 μM, 30 min) treatment (72±6% of basal no peptide for TAT-C24^{615R} and 77±5% of basal no peptide for TAT-C24^{615C}) and had minimal effect on DAT 615C (84±2% of basal no peptide for TAT-C24^{615R} and 85±1% of basal no peptide for TAT- C24^{615C}). Addition of AMPH (10 μM, 30 minutes) to TAT-C24^{R615C} peptide treated DAT 615C cells also did not produce a significant reduction in DA uptake (88±4% basal no peptide control). AMPH addition to TAT-C24^{615C} treated WT-DAT cells significantly blocked AMPH-mediated reduction in the DA transport seen in TAT-C24^{615R} treated and no peptide control conditions (91±3% basal no peptide control). Significant differences were calculated using one-way ANOVA followed by Bonferroni's post hoc test. (n=3–4, P<0.05) **(C)** Presence of DAT 615C or a negatively charged aspartic acid (613E) blocked AMPH-mediated reduction in the DA transport. Specific DA uptake values are expressed as % of basal control. Only DAT 615C (103±13% of basal) and 615E (102±12% of basal) mutations did not display reduction in the DA uptake upon AMPH-treatment (10μM, 30 min). All other mutations at R615 position and DAT 615R showed a significantly reduced DA uptake upon AMPH treatment (615R-68±3%, 615K-75±6%, 615A-66±5%, 615Q-78±5%, 615S-73±5% of basal). Significant differences were calculated using student's t-test for each mutation. (n=3–4, P<0.05) **(D)** Introduction of a negative charge by T613E mutation abolishes AMPH-mediated reduction in the DA transport. AMPH treatment (10 μM, 30 minutes) caused a significant reduction in the DA transport for DAT 615R and 613A (DAT 615R-77±5%, 613A-81±3% of basal) T613E mutation completely blocked AMPH-mediated reduction in the DA transport (97±4% of basal). Mutating T613 to either A or E on DAT 615C background and 615C alone did not produce any significant reduction in the DA uptake upon AMPH treatment (10 μM, 30 minutes) reduction (DAT 615C-92±5%, 613A-615C-86±3%, 613E-615C-92±4% of basal). Significant differences were calculated using student's t-test for each mutation. (n=5, P<0.01)

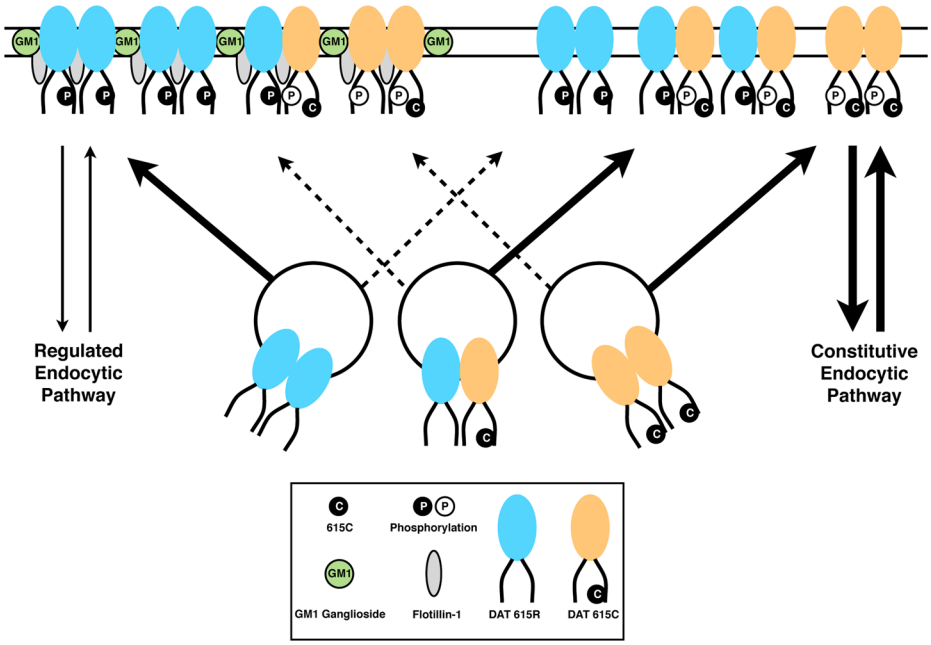

Figure 8. Model describing differential trafficking of DAT 615R and DAT 615C to the regulated and constitutive endocytic pathways and biased localization toward GM1/flotillin-1 rich or depleted membrane microdomains

DAT molecules are depicted as located in trafficking vesicles or at the plasma membrane as homomeric or heteromeric dimers (though other configurations are acceptable). Transporters localize to two types of membrane domains, one domain enriched for GM1 ganglioside and flotillin-1, with the other domain relatively depleted of these molecules. Homo-multimers of WT DAT (615R) subunits target preferentially to GM1 ganglioside/flotillin-1 enriched compartment as compared to DAT 615C subunit containing dimers. The heterodimer is shown preferentially targeting domains that are depleted of GM1 and flotillin-1, in keeping with the dominant action of the 615C mutation in the ADHD proband and the dominant action of the DAT C-terminal peptide containing 615C. DAT 615C subunits are diminished in surface levels relative to WT subunits. Microdomains enriched for GM1 and flotillin-1 support regulated trafficking of DATs, and under basal conditions exhibit slow rates of endocytosis, whereas membranes depleted of GM-1 and flottilin-1 support more rapid, constitutive endocytosis and recycling.